Organic & Biomolecular Chemistry

Dynamic Article Links

Cite this: *Org. Biomol. Chem.*, 2012, **10**, 597

www.rsc.org/obc

PAPER

Origins of enantioselectivity in the chiral diphosphine-ligated CuH-catalyzed asymmetric hydrosilylation of ketones†

Wei Zhang, Weiyi Li and Song Qin*

Received 29th August 2011, Accepted 12th October 2011
DOI: 10.1039/c1ob06478a

Computational investigations on the asymmetric hydrosilylation of acetophenone over ligated CuH catalysts were performed with the DFT method. The calculations predict that the catalytic reaction involves two steps: (1) CuH addition to the carbonyl group *via* a four-membered transition state (TS) with the formation of copper-alkoxide intermediates; (2) regeneration of the ligated CuH catalyst by an external SiH_4 through a metathesis process to yield the corresponding silyl ether. The calculations in the chiral diphosphine-ligated CuH systems suggest that the metathesis process is the rate-determining step (RDS). The CuH addition step is vital for the distribution of the racemic products and therefore represents the stereo-controlling step (SCT). In this step, the greater steric hindrance between the aromatic rings of the ligands and the substrate is identified as the major factor for enantioselectivity. The corresponding TS in the face-to-face mode, suffering less steric hindrance, is more stable than its analogue in the edge-to-face mode. The enantioselectivities are calculated to be related not only to the P–Cu–P bite angles in the stereo-controlling TSs, but also to the substituents at the P-aryl rings of the chiral ligands. In short, a larger P–Cu–P bite angle and suitably modified P-aryl rings together are necessary to achieve excellent ee values.

1. Introduction

Asymmetric reduction of carbonyl compounds is an important protocol in organic synthesis, because this reaction is an effective method to obtain chiral nonracemic secondary alcohols, providing significant intermediates in the manufacture of pharmaceutical products and advanced materials.[1] Transition-metal catalysis has been successfully applied in the reduction of many carbonyl compounds *via* hydrogenation or hydrosilylation.[2] In recent years, numerous transition-metal catalysts, such as rhodium,[3] titanium,[4] iron,[5] zinc,[6] copper[7] *etc.*, have been developed in asymmetric hydrogenation/hydrosilylation of carbonyl compounds with high yields and enantiomeric excess (ee) values. Among these metal catalysts, copper-based systems have been proven to be the most attractive candidate for the asymmetric hydrosilylation, since copper-systems exhibit remarkable merits, *i.e.* economical and environmentally benign, practical, cheaper and less toxic. Notably, the benefits of copper hydride catalysis include advantages for synthesis, *i.e.* high levels of enantiomeric excess, high yields, easy to handle, considerable tolerance to a variety of functional groups.

In asymmetric hydrosilylation reactions, copper-hydride species combined with diphosphine ligands exhibit good to excellent catalytic performances (Scheme 1). In 1984, Brunner and Miehling published an article on asymmetric hydrosilylation with a CuH/phosphine system.[8] They reported that copper catalysts in a mixture of Cu(I) compounds and optically active chelate phosphines [(–)Diop, (+)Norphos, (–)BPPFA] could afford optical yields of 10–40% ee for the quantitative hydrosilylation of acetophenone with diphenylsilane.

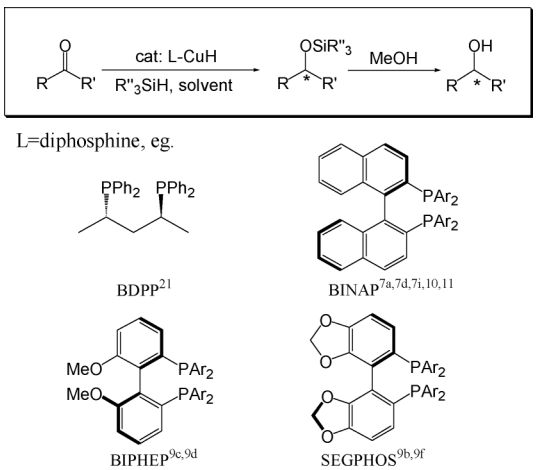

Scheme 1 Typical diphosphine ligands used in CuH-catalyzed hydrosilylation reactions.

Since then, a great improvement was accomplished by Lipshutz and co-workers. They reported a great many asymmetric

Key Laboratory of Green Chemistry and Technology, Ministry of Education, College of Chemistry, Sichuan University, Chengdu, Sichuan, 610064, China. E-mail: qinsong@scu.edu.cn

† Electronic supplementary information (ESI) available: Computational methods, energies, optimized geometries and the full citation of Gaussian 03 program. See DOI: 10.1039/c1ob06478a

hydrosilylation reactions catalyzed by chiral phosphine-ligated copper hydride with competitive yields and ee values.[9] They proposed that the coordination of diphosphine ligands to copper hydride made this species more reactive and efficient. In their work, diphosphine ligands, such as BINAP, MeO-BIPHEP, SEGPHOS, have been successfully introduced into CuH-catalyzed asymmetric hydrosilylation reactions. Lipshutz *et al.* reported that MEO-BIPHEP-CuH complexes or SEGPHOS-CuH complexes can catalyze enantiomeric hydrosilylation of aromatic ketones at low temperature (−78 °C) with high ee values up to 96%, and substrate-to-ligand ratios exceeding 100 000 : 1 can also be obtained. Sirol *et al.*[10] introduced a base-free and air-accelerated system: CuF_2/(*R*)-BINAP/$PhSiH_3$, which furnished secondary alcohols with moderate to good enantiomeric excess values under ambient conditions. Lee *et al.*[11] developed a novel method of generating the copper hydride catalyst with an easy-to-handle copper source. The air and moisture stable Cu(II) salt $Cu(OAc)_2 \cdot H_2O$ has been found to be comparably reactive to the combination of CuCl/NaOtBu and resulted in increased reaction rates. These efforts contributed to this field have received remarkable success in terms of improving the reaction conditions and enhancing the yields and ee values.

For the mechanism of the copper-catalyzed hydrosilylation reaction, a catalytic cycle involving two steps is available in the literature (Scheme 2). In the first step, copper hydride interacts with the ketone to form a copper alkoxide. In the second step, the copper alkoxide intermediate undergoes a σ-bond metathesis with silanes to produce the silyl ether with the regeneration of the CuH catalyst. Lee *et al.*[11] suggested that this mechanism was consistent with their observations. They found that the organosilanes affected the reaction rates but not the enantioselectivity of products. More recently, Gathy *et al.*[12] performed a computational investigation on the mechanism of formaldehyde hydrosilylation over nonchiral copper-based catalysts. The proposed mechanism was also compatible with the experimental presumption.

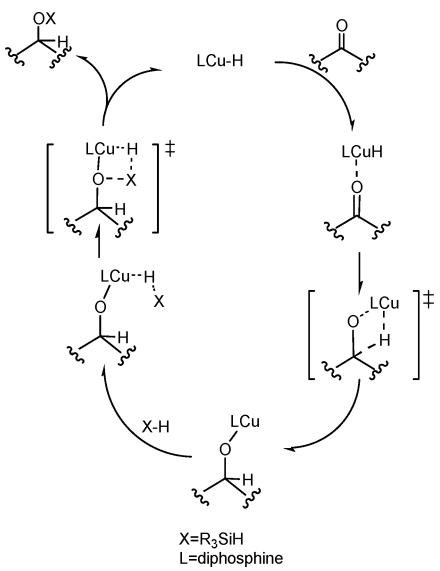

Scheme 2 Proposed catalytic cycle of CuH-catalyzed hydrosilylation of ketones.

The detailed mechanism of such a copper-catalyzed hydrosilylation of ketones, as well as the origin of the stereochemistry, however, is much less known. Although it is well known that the chiral environment is controlled by classical steric and electronic factors and the rigidity of the ligand framework,[13] the effects of chiral ligands on such asymmetric reactions are still uncertain. Therefore, it is hard to precisely evaluate the important parameters of chiral ligands associated with high ee values, which becomes an obstacle for designing new effective chiral ligands. The present investigation focuses on the origin of the stereochemistry of asymmetric hydrosilylation of prochiral ketones. In an attempt to gain a better understanding of the underlying steps of the hydrosilylation reaction at a molecular level and to clarify how the chiral diphosphine-ligated copper hydride catalysts enhance the reaction enantioselectivity, we here carry out theoretical simulations on such reaction systems.

2. Models and computational details

In the present investigation, the simulated reaction is shown in Scheme 3. The catalyst models used in the present calculations could be classified into the following two categories. Here, SiH_4 was used as the silylating agent and acetophenone as the substrate.

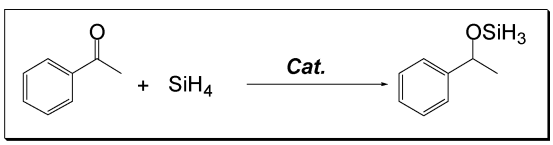

Cat:* *Model 1: CuH diatomic molecule
Model 2: L-CuH(L=L$_1$-L$_3$*)

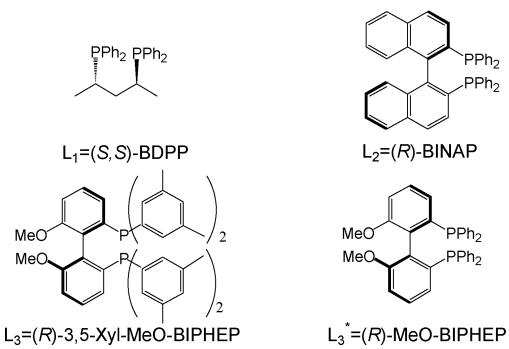

Scheme 3 Typical diphosphine ligands used in CuH-catalyzed hydrosilylation reactions.

2.1 Diatomic CuH model

The diatomic molecule CuH in the ground state of $^1\Sigma$ was used as a simple catalyst model in the above reaction. Although the real reactions were performed in the condensed phase, such a simple model is expected to provide some information about the reaction mechanism and can be the foundation of the following calculations in the ligated systems. In this section, the structural optimizations of all the intermediates (IM) and transition states (TS) were performed using Becke's three parameter exchange functional and the nonlocal correlation functional of Lee, Yang and Parr (B3LYP)[14] with the 6-31+G(d,p) basis set[15] for all atoms. In order to evaluate the sensibility of the results to basis sets, the geometries of the located stationary points were re-optimized at the B3LYP/6-311++G(2d,2p) level. This benchmark indicates that the potential

energy surfaces at the two levels are quite close to each other. With the combination of previous computational literature which demonstrate that the B3LYP method performs well for copper systems,[16] the calculations at the B3LYP/6-31+G(d,p) level might be suitable for the present CuH-catalyzed reactions.

2.2 Ligated CuH models

In this section, the reaction systems based on chiral diphosphine ligands were introduced in the present simulation (Scheme 3, L_1–L_3 were used as the actual ligands in the experiments). Because the experimental evidence supported that the diphosphine–CuH complexes should be in the monomeric form,[7m,9d] the monomeric ligated CuH species were constructed as the catalysts in this section. To reduce computational costs, the calculations are performed with the B3LYP/gen method (3-21G** basis sets being employed for the moieties of the above ligands except for P atoms; 6-31+G(d,p) basis sets for the rest at the B3LYP level). To take the entropy effects into account, the following discussion is based on the Gibbs free energies of reaction. As toluene was often used as the solvent in experiments,[7h] the latter calculations were carried out with a dielectricity constant $\varepsilon = 2.379$ for the solvent toluene. For evaluating the solvent effects, single-point self-consistent reaction field (SCRF) calculations based on the polarized continuum model (PCM)[17] were carried out on the optimized geometries for all species at the B3LYP/gen level. The solvation free energy was calculated at the B3LYP/6-31+G(d,p) level and added to the gas-phase free energy to obtain the Gibbs free energy in toluene (G_{solv}) at 298.15 K, with radii = UAHF. Unless otherwise stated, the G_{solv} is used in the discussion and the energy curves refer to the G_{solv} scale. For the BDPP system, all IMs and TSs along the entire reaction route were located on the potential energy surface (PES). For the other chiral ligated systems, only the stereo-controlling TSs were optimized at the same level.

All calculations were performed with the Gaussian 03 programs.[18] Frequencies were calculated at the same level to confirm each stationary point to be either a minimum (no imaginary frequency) or a saddle point (unique imaginary frequency), and to obtain the zero-point correction.

3. Results and discussion

3.1 Hydrosilylation catalyzed by diatomic CuH molecule

The corresponding optimized structures and the energy diagrams along the predicted reaction path are depicted in Fig. 1 and 2.

As shown in Fig. 1, the calculations feature a two-step catalytic cycle in the CuH/acetophenone/SiH_4 system: (1) CuH addition step: a diatomic CuH molecule coordinates to acetophenone with the formation of the precursor complex **COM1**. Then, the hydrogen atom of CuH migrates to the carbon atom of the carbonyl moiety *via* a four center transitional state **TS1**, generating a copper-alkoxide intermediate **IM1**, (2) regeneration of CuH catalyst: **IM1** interacts with an external SiH_4, followed by the metathesis process to yield the corresponding silyl ether with concomitant regeneration of the CuH catalyst. The above results are generally compatible with the mechanism of formaldehyde hydrosilylation proposed by Gathy *et al.*[12]

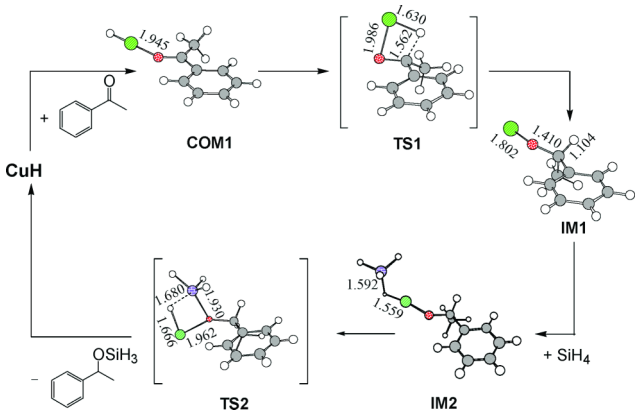

Fig. 1 Optimized structures of all intermediates and transition states in the simple CuH/acetophenone/SiH_4 system.

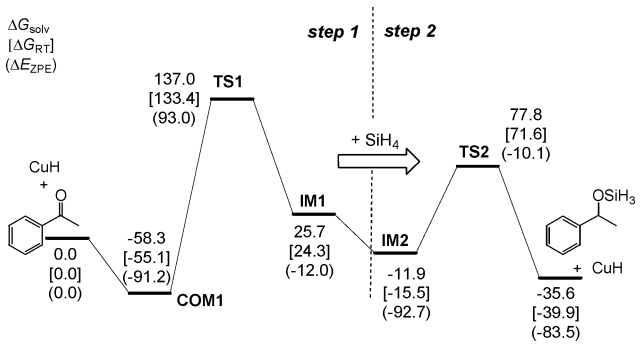

Fig. 2 Energy diagram along the reaction route in the simple CuH/acetophenone/SiH_4 system. Relative energies (in kJ mol^{-1}) for various species are calculated at the B3LYP/6-31+G(d,p) level. (ΔG_{RT}: Gibbs free energies in the gas-phase; ΔG_{solv}: Gibbs free energies in toluene; ΔE_{ZPE}: ZPE-corrected electronic energies).

As shown in Fig. 2, regardless of the ΔG_{solv}, ΔG_{RT} or ΔE_{ZPE}, the first reaction step possesses the largest energy barrier, which indicates that the CuH addition step *via* **TS1** might be the rate-determining step (RDS) for the overall reaction. The inclusion of the solvent effect induced by toluene exerts a little influence on the energy barriers, suggested by the smaller discrepancy (<6.2 kJ mol^{-1}) between ΔG_{solv} and ΔG_{RT} on the PES. On the other hand, the calculations give a ΔE_{ZPE} much different from ΔG_{RT} and ΔG_{solv}, which might be caused by the exclusion of entropic or solvent effects.

It should be noted that there are no experiments directed to such a simple diatomic CuH system in the literature, which makes the precise comparison with experimental observations less meaningful. For the ligated CuH catalysts actually used in solution experimentally, the simulations on 'actual' systems in the condensed phase is necessary and therefore performed in the next section.

3.2 Hydrosilylation catalyzed by BDPP-CuH complexes

The optimized structures along the predicted reaction paths and the energy diagrams in the BDPP-CuH system are depicted in Fig. 3 and Fig. 4, respectively. As shown in Fig. 3, in the L_1-CuH catalyst, the BDPP(L_1) bonds with the copper center by its P-ends with P–Cu lengths of 2.311 Å and 2.347 Å, respectively, and the CuH

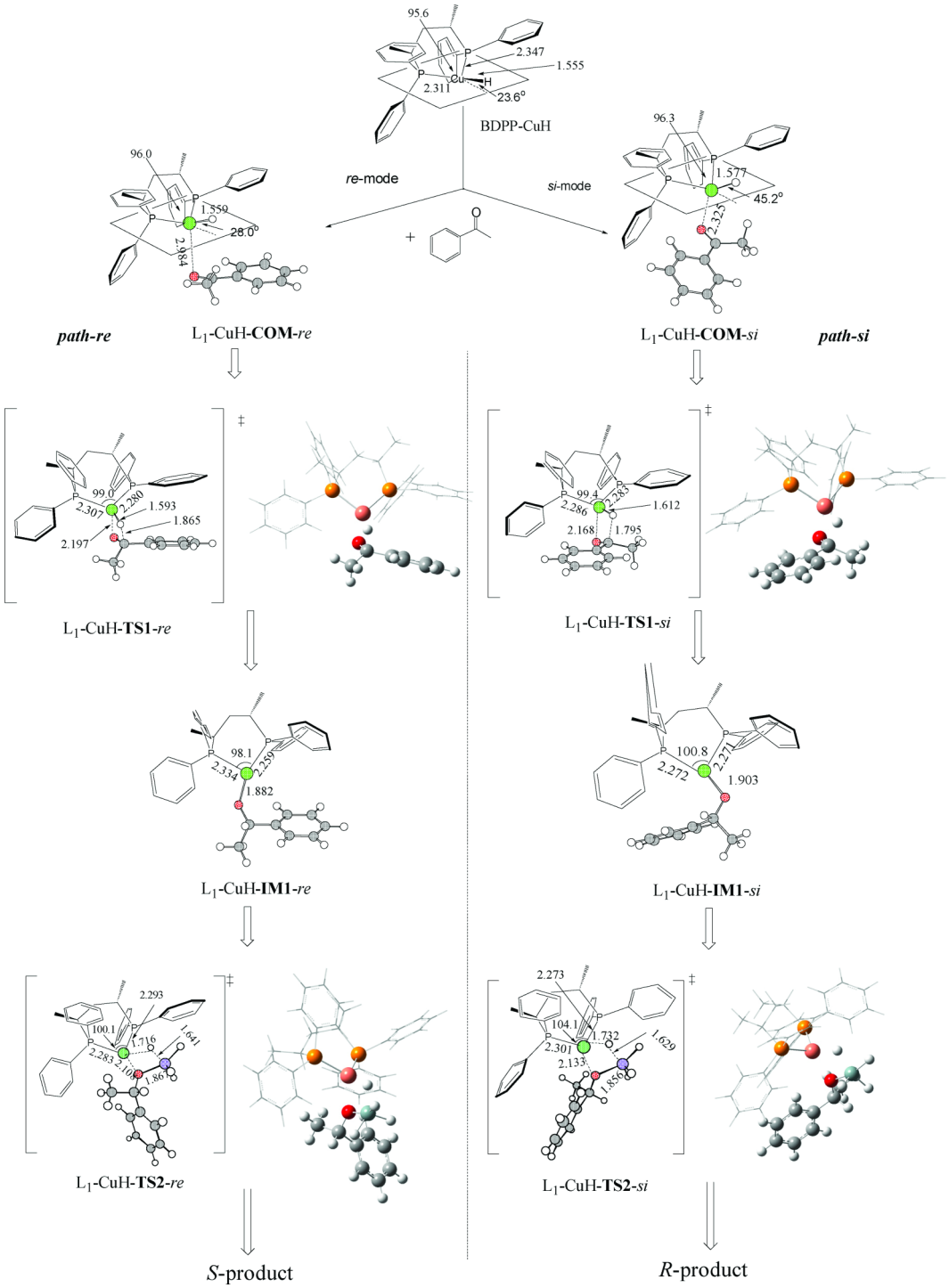

Fig. 3 Optimized intermediates and transition states in the L_1-CuH/acetophenone/SiH_4 system. Bond lengths are in Å, and bond angles are in degrees.

bond is slightly out of the P–Cu–P plane with a distorted angle θ of 23.6°. Next, the coordination of L_1–CuH to acetophenone can alternatively occur from the *re* or *si* face of the substrate with the formation of catalyst–acetophenone complexes. Since L_1 possesses C_2-symmetry, two L_1-CuH-acetophenone complexes (L_1-CuH-**COM**-*re*, L_1-CuH-**COM**-*si*) different in the orientation of acetophenone to the L_1-CuH catalyst result from the above coordination process.

In L_1-CuH-**COM**-*re*, the L_1-CuH moiety is located on the *re*-side of acetophenone with a Cu–O distance of 2.984 Å. The Cu–H moiety is further distorted out of the P–Cu–P plane with an angle of 28.0°, and the Cu–H bond length is slightly elongated to 1.559 Å. In contrast, for L_1-CuH-**COM**-*si*, the L_1-CuH moiety is on the *si*-side of acetophenone with a Cu–O distance of 2.325 Å. The Cu–H moiety is drastically distorted out of the P–Cu–P plane with a larger angle of 45.2°, and the corresponding

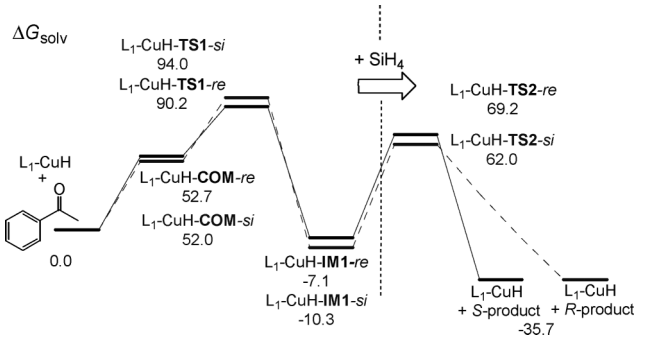

Fig. 4 Energy diagrams along the reaction routes in the L_1-CuH/acetophenone/SiH_4 system. The relative Gibbs free energies in the solvent (ΔG_{solv}) at the B3LYP(PCM)/6-31+G(d,p) level are in kJ mol^{-1}.

Cu–H bond is elongated to 1.577 Å. The following reaction can take place from L_1-CuH-**COM**-*re* or L_1-CuH-**COM**-*si*, and the corresponding reaction routes are marked as path-*re* or path-*si*, respectively.

Reaction path-*re*. From L_1-CuH-**COM**-*re*, the addition of CuH into the carbonyl from the *re* face with the cleavage of the Cu–H bond takes place *via* L_1-CuH-**TS1**-*re*, leading to an *S*-configuration copper-alkoxide intermediate L_1-CuH-**IM1**-*re*. L_1-CuH-**TS1**-*re* is a four-membered cyclic transition state with an elongated C═O bond of 1.284 Å and a shortened C–H bond of 1.865 Å. Notably, the phenyl ring of acetophenone in L_1-CuH-**TS1**-*re* is nearly parallel with the equatorial P-aryl ring (aryl ring at the phosphorus atom), which features L_1-CuH-**TS1**-*re* in the face-to-face mode. After L_1-CuH-**TS1**-*re*, the C–H distance shortens to 1.110 Å in L_1-CuH-**IM1**-*re*, indicating the completion of the addition of the CuH moiety to the carbonyl group. PCM calculations predict the Gibbs energy barrier ($\Delta G^{\neq}_{solv}$) of this step to be 37.5 kJ mol^{-1}.

The second step is the recovery of the L_1-CuH catalyst by an external SiH_4 *via* L_1-CuH-**TS2**-*re*. In this step, the hydrogen of SiH_4 migrates to the copper center *via* a four-membered transition state L_1-CuH-**TS2**-*re*, followed by the release of the final product. L_1-CuH-**TS2**-*re* features the factors: the Cu–H bond has already been formed, while the O–Si bond formation is on the way and the Cu–O bond begins to elongate.

Finally, the *S*-configuration product is yielded with the recovery of the L_1-CuH catalyst. PCM calculations predict the energy barrier ($\Delta G^{\neq}_{solv}$) for the second step to be 76.3 kJ mol^{-1} in Gibbs free energies.

Reaction path-*si*. There exists another reaction route path-*si* similar to the path-*re* in mechanism. Along this reaction route, the chiral L_1-CuH catalyst gets close to acetophenone from the *si* face to generate an *R*-configuration copper-alkoxide intermediate L_1-CuH-**IM1**-*si* *via* L_1-CuH-**TS1**-*si*. In L_1-CuH-**TS1**-*si*, the equatorial P-aryl ring at the phosphorus atom and the phenyl ring of acetophenone are in the edge-to-face mode. After L_1-CuH-**TS1**-*si*, the C–H bond shortens to 1.112 Å in L_1-CuH-**IM1**-*si*. Next, the recovery of L_1-CuH by the external SiH_4 occurs, leading to the formation of the final product in the *R*-configuration. The properties of PES along the path-*si* are comparable with that along the path-*re*. The CuH addition TS (L_1-CuH-**TS1**-*si*) along path-*si* possesses an energy barrier of 42.0 kJ mol^{-1}.

Compared with the simple diatomic CuH system, the Gibbs energy barrier at **TS1** is dramatically dropped to *ca.* 40 kJ mol^{-1} in the L_1-CuH catalytic system. These results suggest that the ligated CuH complexes decrease the energy barrier and exhibit a better catalytic performance for the hydrosilylation of ketones. NBO[19] analysis predicts that the charge accumulated at the Cu atom in the BDPP-ligated CuH system changes more moderately than that in the simple diatomic CuH system (Fig. 5). Especially, the charge at the Cu atom is *ca.* 0.7 e in L_1-CuH-**TS1**s, significantly more negative than that in the simple CuH-**TS1** species (0.843 e). This might be caused by the chelation effect in which the two phosphorus atoms make the CuH catalyst accept more negative charge. With such electronic properties, the electrophilic carbonyl group prefers to interact with the diphosphine-ligated CuH catalyst, and therefore the energy barrier of the CuH addition process decreases in the ligated CuH system.

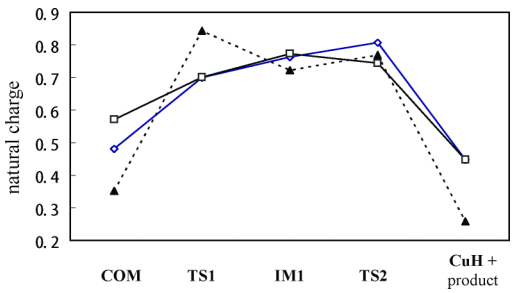

Fig. 5 Charge at the Cu atom changes in the hydrosilylation reaction. (▲: CuH gas-phase system; □: path-*si* in BDPP-CuH system; ◇: path-*re* in BDPP-CuH system).

Distribution of final products. As shown in Fig. 4, the second step *via* **TS2** possesses the largest energy barrier along each reaction path, implying that the metathesis process might be the rate-determining step (RDS) for the BDPP-CuH-catalyzed reaction.

However, according to the Curtin–Hammett principle,[20] the evolution of the most stable intermediate **IM1** is vital for the distribution of final products. As shown in Fig. 4, the reverse energy barrier from **IM1** to **COM** *via* **TS1** is much larger than the forward one *via* **TS2**, which means that the first reaction step should be irreversible. The above result indicates that the first reaction step is responsible for the enantioselectivity and the second step is related to the reaction rates. This could interpret the experimental observations of Lipshutz's group[9d] and Lee's group[11] that the organosilanes affected the reaction rates but not the enantioselectivity of product.

L_1-CuH-**TS1**-*re* along the reaction path-*re* is 3.8 kJ mol^{-1} lower than its analogue L_1-CuH-**TS1**-*si* along path-*si* in Gibbs free energies, which means that the major product should be in the *S*-configuration. According to the Boltzmann distribution, the theoretically predicted ee for the corresponding *S*-product is 64% in the present calculations. Although this theoretical prediction overestimates the 40–56% ee of the *S*-product in experiments,[21] the present calculations successfully reproduce the correct major product.

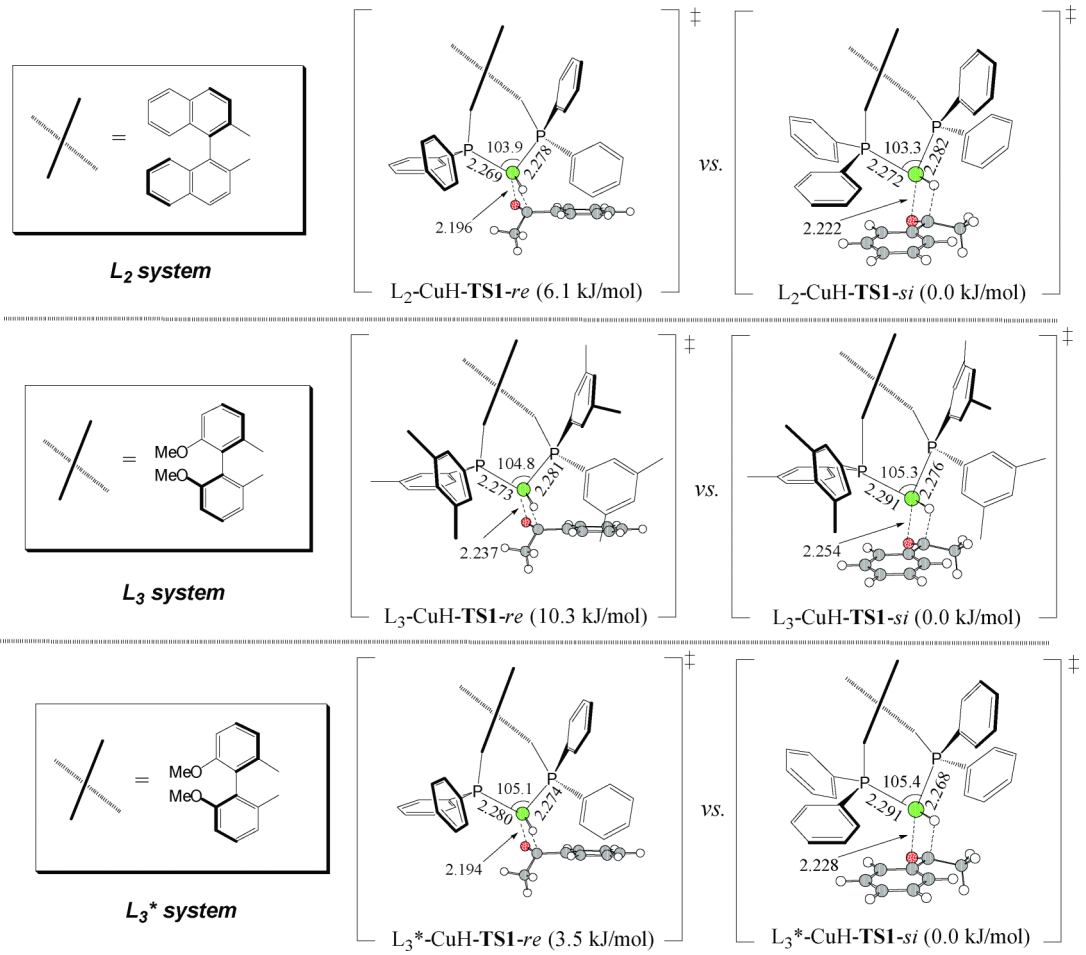

Fig. 6 Optimized intermediates and transition states in the L_2–L_3* systems. Bond lengths are in Å, and bond angles are in degrees.

3.3 Simulation on the other chiral systems

To evaluate the computational accuracy in the tested reaction, two actually used ligands (L_2 and L_3, see computational details) were also introduced in the following calculations. As mentioned above, the distribution of the final products is determined in the first reaction step (CuH addition step). Therefore, to reduce computational costs, the following investigations on the stereochemistry of these ligated systems will focus on the structures of CuH addition transition states L-CuH-**TS1**s. The optimized L-CuH-**TS1**s are provided in Fig. 6. Similar to the L_1-CuH system, these ligated-CuH catalysts also possess a gross structure of a P–Cu–P network. For these ligands of C_2-symmetry, two attack modes for the CuH catalyst to the substrate result: the catalyst could attack acetophenone from the *re* face to give the product in an *S*-configuration; while the catalyst could attack acetophenone from the *si* face to generate the product in the *R*-configuration.

For the L_2 and L_3 ligand systems, the competing TSs can be distinguished from each other by the location of the phenyl ring of acetophenone with respect to the ligand. In L_2- and L_3-CuH-**TS1**-*si*, the phenyl ring of acetophenone is in the face-to-face mode to the equatorial P-aryl ring with the formation of a parallel displaced configuration.

In contrast, the phenyl ring of acetophenone and the equatorial P-aryl ring are located in the edge-to-face mode in L_2- and L_3-CuH-**TS1**-*re*, which might generate a considerable repulsion between the substrate and the ligand. Therefore, the larger steric hindrance between the P-aryl ring of the ligands and the phenyl ring of the substrate might be the original reason for the stereochemistry of the reaction. The TSs in the face-to-face mode are thermodynamically more stable than those in the edge-to-face mode.

PCM calculations indicate that L_2- and L_3-CuH-**TS1**-*si* in the face-to-face mode is *ca.* 4–10 kJ mol^{-1} more stable than its analogue L_2- and L_3-CuH-**TS1**-*re*. Table 1 summaries the PCM energy gaps ($\Delta G^{\neq}_{g,solv}$) of these TSs at the B3LYP(PCM)/6-31+G(d,p) level and the experimental results. Although the calculated $\Delta G^{\neq}_{g,solv}$ for L_1–L_3 are slightly overestimated compared to experimental values, the predictions are correct for the major product. These results indicate that the present calculations are reasonable.

3.4 Effect of the ligand structure on the stereochemistry

As shown in Table 2, for the actually used L_1–L_3 systems, the ee value has a positive relationship with the P–Cu–P bite angle in either the favoured **TS1** or the disfavoured one. The higher ee values are observed in the systems with the larger bite angle in general. For example, in the favoured **TS1**s, the bite angles are 99.0° in L_1, 103.3° in L_2, 105.3° in L_3. Correspondingly, the calculated and experimental ee values exhibit the same trend

Table 1 Relative Gibbs free energy gaps ($\Delta G^{\neq}_{g,solv}$, in kJ mol^{-1}) at the B3LYP(PCM)/6-31+G(d,p) level for the L_1–L_3* systems

Ligand	Cal. $\Delta G^{\neq}_{g,solv}$	Exp. $\Delta G^{\neq}_{g}$	Exp. ee (%)
L_1	−3.8	−3.1	56(*S*)[21]
L_2	6.1	4.7	74(*R*)[9d]
L_3	10.3	8.6	94(*R*)[9d]
L_3*	3.5	—	—

*$\Delta G^{\neq}_{g,solv} = G^{\neq}_{solv}$ (**TS1**-*re*) − $G^{\neq}_{solv}$ (**TS1**-*si*). Occupied probability based on the Boltzmann distribution, $N_i/N = [g_i\exp(-G_i/kT)]/[\Sigma g_i\exp(-G_i/kT)]$ (T = 298.15 K). ee = $|(R - S)|/(R + S)$.

Table 2 Calculated P–Cu–P bite angles *versus* experimental enantioselectivities

Ligand	θ in favoured **TS1**	θ in disfavoured **TS1**	Exp. $\lvert\Delta G^{\neq}_{g}\rvert$ (kJ mol^{-1})
L_1	99.0	99.4	3.1
L_2	103.3	103.9	4.7
L_3	105.3	104.8	8.6
L_3*	105.4	105.1	—

for the L_1 to L_3 systems. In other asymmetric catalytic reactions catalyzed by metal-complexes of C_2-symmetry, bite angles roughly related to the stereochemistry have been documented,[22] but the full reason for this apparent phenomenon is still uncertain.

It should be emphasized that L_3 is associated with the largest P–Cu–P bite angle, but it possesses dimethyl residues at the P-aryl rings, which is much different from L_1 and L_2. To understand the role of the substituents on the P-aryl rings, L_3* was constructed and used in the simulation (see Scheme 3). The calculated energy gap $\Delta G^{\neq}_{g,solv}$ for the L_3* system is rather low (3.5 kJ mol^{-1}) when compared to that of the L_3 system (10.3 kJ mol^{-1}), which means that the ligand with the substituents on the P-aryl rings has a more remarkable chiral induction in such hydrosilylation reactions.

As shown in Fig. 6, the bite angles in the L_3 and L_3* systems are almost the same (105.3° *versus* 105.4° in the favoured **TS1**), suggesting that the bite angle is sensitive to the framework of the ligand rather than the substituents on the P-aryl rings.

Apart from the bite angles, the impact of the substituents on the P-aryl rings on the enantioselectivity was also observed in other ligated metal-catalyzed reactions.[23] Pregosin *et al.* explained the diaryl *meta* effect for MeO-BIPHEP complexes related to Heck, allylic alkylation and hydrogenation reactions.[23a,23c] They supposed that one of the two 3,5-dimethyl P-aryl rings interacts selectively with the remaining ligand, and then, the entire chiral pocket becomes slightly more rigid and the correlation with substrate improves. On the basis of related experimental results with other metal-catalyzed systems reported by other groups and copper complexes calculated by our group, it could be deduced that the dialkyl *meta* effect on enantioselectivity has some generality in enantioselective catalysis.

In the present investigation, the apparent relationship between the structural parameters and enantioselectivities is rationalized for the titled reaction. The high ee values are not only associated with larger bite angles, but are also dependent on the structure of the P-aryl ring moieties. These two structural parameters together control the enantioselectivity of the reactions. The advantageous parameters for good enantioselectivities include: (1) larger bite angles in the biaryl diphosphine-complexed copper hydride; (2) a diphosphine ligand with substituted P-aryl rings is more preferable than a ligand with P-phenyl rings.

4. Conclusions

The calculations indicate that the mechanism of ketone hydrosilylation is composed of two steps: (1) CuH addition to the carbonyl group: ligated copper hydride coordinates to acetophenone, followed by the addition of the hydrogen atom to the double bond of carbonyl moiety *via* a four-membered transition state with the formation of copper-alkoxide intermediates, (2) regeneration of ligated CuH catalysts by an external SiH_4: the copper-alkoxide interacts with SiH_4 through a metathesis process to yield the corresponding silyl ether. In the diphosphine ligand systems, the distribution of the final products should be closely dependent on the CuH addition step *via* **TS1**, and therefore this step is stereo-controlling. The introduction of the ligand, such as BDPP, dramatically decreases the energy barrier in the CuH addition step, suggesting that the ligated CuH-catalyzed reaction might be ligand-accelerated. The larger steric hindrance between the P-aryl rings of the ligands and the phenyl ring of the substrate might be the original reason for the stereochemistry of the reaction. The **TS1** in the face-to-face mode, suffering less steric hindrance, is much more stable than its competing TS in the edge-to-face mode. Furthermore, the P–Cu–P bite angle and the substituents on the P-aryl rings are both key structural parameters controlling the enantioselectivity of the copper-catalyzed hydrosilylation.

Acknowledgements

The authors are grateful for financial support from the National Science Foundation of China (Nos. 20772085, 21021001 and 20732030).

References

1 E. J. Corey and C. J. Helal, *Angew. Chem., Int. Ed.*, 1998, **37**, 1986–2012.
2 (*a*) S. Díez-Gonázlez and S. P. Nolan, *Acc. Chem. Res.*, 2007, **41**, 349–358; (*b*) B. Marciniec, H. Maciejewski, C. Pietraszuk and P. Pawluć, *In Advances in Silicon Science, Vol 1: Hydrosilylation A Comprehensive Review on Recent Advances*, Springer, Berlin, 2009, vol. 1, chapter 10.1, pp. 342–382.
3 (*a*) L. H. Gade, V. César and S. Bellemin-Laponnaz, *Angew. Chem., Int. Ed.*, 2004, **43**, 1014–1017; (*b*) A. G. Coyne and J. G. Patrick, *Tetrahedron Lett.*, 2007, **48**, 747–750; (*c*) O. Pàmies, C. Claver and M. Diéguez, *J. A. Mol. Phys.*, 2006, **249**, 207–210; (*d*) V. César, S. Bellemin-Laponnaz, H. Wadepohl and L. H. Gade, *Chem.–Eur. J.*, 2005, **11**, 2862–2873; (*e*) D. Cuervo, M. P. Gamasa and J. Gimeno, *J. A. Mol. Phys.*, 2006, **249**, 60–64; (*f*) N. Schneider, M. Finger, C. Haferkemper, S. Bellemin-Laponnaz, P. Hofmann and L. H. Gade, *Angew. Chem., Int. Ed.*, 2009, **48**, 1609–1613; (*g*) N. Schneider, M. Finger, C. Haferkemper, S. Bellemin-Laponnaz, P. Hofmann and L. H. Gade, *Chem.–Eur. J.*, 2009, **15**, 11515–11529.
4 (*a*) M. B. Carter, B. Schøitt, A. Gutiérrez and S. L. Buchwald, *J. Am. Chem. Soc.*, 1994, **116**, 11667–11670; (*b*) R. L. Halterman, T. M. Ramsey and Z. L. Chen, *J. Org. Chem.*, 1994, **59**, 2642–2644; (*c*) J. Yun and S. L. Buchwald, *J. Am. Chem. Soc.*, 1999, **121**, 5640–5644.
5 (*a*) N. S. Shaikh, S. Enthaler, K. Junge and M. Beller, *Angew. Chem., Int. Ed.*, 2008, **47**, 2497–2501; (*b*) A. M. Tondreau, L. Lobkovsky and P. J. Chirik, *Org. Lett.*, 2008, **10**, 2789–2792; (*c*) J. Yang and T. D. Tilley, *Angew. Chem., Int. Ed.*, 2010, **49**, 10186–10188; (*d*) T. Inagaki, A. Ito, J. Ito and H. Nishiyama, *Angew. Chem., Int. Ed.*, 2010, **49**, 9384–9387.
6 (*a*) V. Bette, A. Mortreux, D. Savoia and J. F. Carpentier, *Adv. Synth. Catal.*, 2005, **347**, 289–302; (*b*) H. Mimoun, J. Y. S. Laumer, L. Giannini, R. Scopelliti and C. Floriani, *J. Am. Chem. Soc.*, 1999, **121**, 6158–6166.

7 (*a*) M. L. Kantam, S. Laha, J. Yadav, P. R. Likhar, B. Sreedhar and B. M. Choudary, *Adv. Synth. Catal.*, 2007, **349**, 1797–1802; (*b*) X. C. Zhang, Y. Wu, F. Yu, F. F. Wu, J. Wu and A. S. C. Chan, *Chem.–Eur. J.*, 2009, **15**, 5888–5891; (*c*) T. Fujihara, K. Semba, J. Terao and Y. Tsuji, *Angew. Chem., Int. Ed.*, 2010, **49**, 1472–1476; (*d*) M. L. Kantam, J. Yadav, S. Laha, P. Srinivas, B. Sreedhar and F. Figueras, *J. Org. Chem.*, 2009, **74**, 4608–4611; (*e*) W. J. Li and S. X. Qiu, *Adv. Synth. Catal.*, 2010, **352**, 1119–1122; (*f*) K. Junge, B. Wendt, D. Addis, S. Zhou, S. Das and M. Beller, *Chem.–Eur. J.*, 2010, **16**, 68–73; (*g*) S. Rendler and M. Oestreich, *Angew. Chem., Int. Ed.*, 2007, **46**, 496–504; (*h*) C. Deutsch, N. Krause and B. H. Lipshutz, *Chem. Rev.*, 2008, **108**, 2916–2927; (*i*) J. T. Issenhuth, S. Dagorne and S. Bellemin-Laponnaz, *C. R. Chim.*, 2010, **13**, 353–357; (*j*) J. Wu, J. X. Ji and A. S. C. Chan, *Proc. Natl. Acad. Sci. U. S. A.*, 2005, **102**, 3570–3575; (*k*) S. Díez-González, E. D. Stevens, N. M. Scott, J. L. Petersen and S. P. Nolan, *Chem.–Eur. J.*, 2008, **14**, 158–168; (*l*) J. T. Issenhuth, S. Dagorne and S. Bellemin-Laponnaz, *Adv. Synth. Catal.*, 2006, **348**, 1991–1994; (*m*) D. H. Appella, Y. Moritani, R. Shintani, E. M. Ferreira and S. L. Buchwald, *J. Am. Chem. Soc.*, 1999, **121**, 9473–9474.

8 H. Brunner and W. Miehling, *J. Organomet. Chem.*, 1984, **275**, C17–C21.

9 (*a*) B. H. Lipshutz, W. Chrisman and K. Noson, *J. Organomet. Chem.*, 2001, **624**, 367–371; (*b*) B. H. Lipshutz, C. C. Caires, P. Kuipers and W. Chrisman, *Org. Lett.*, 2003, **5**, 3085–3088; (*c*) B. H. Lipshutz, K. Noson and W. Chrisman, *J. Am. Chem. Soc.*, 2001, **123**, 12917–12918; (*d*) B. H. Lipshutz, K. Nosan, W. Chrisman and A. Lower, *J. Am. Chem. Soc.*, 2003, **125**, 8779–8789; (*e*) C. T. Lee and B. H. Lipshutz, *Org. Lett.*, 2008, **10**, 4187–4190; (*f*) B. H. Lipshutz, A. Lower, R. J. Kucejko and K. Noson, *Org. Lett.*, 2006, **8**, 2969–2972; (*g*) B. H. Lipshutz, A. Lower and K. Noson, *Org. Lett.*, 2002, **4**, 4045–4048.

10 S. Sirol, J. Courmarcel, N. Mostefai and O. Riant, *Org. Lett.*, 2001, **3**, 4111–4113.

11 D. W. Lee and J. Yun, *Tetrahedron Lett.*, 2004, **45**, 5415–5417.

12 T. Gathy, D. Peeters and T. Leyssens,, *J. Organomet. Chem.*, 2009, **694**, 3943–3950.

13 H. Shimizu, I. Nagasaki and T. Saito, *Tetrahedron*, 2005, **61**, 5405–5432.

14 (*a*) A. D. Becke, *J. Chem. Phys.*, 1993, **98**, 5648–5652; (*b*) C. Lee, W. Yang and R. G. Parr, *Phys. Rev. B*, 1998, **37**, 785–789; (*c*) B. Miehlich, A. Savin, H. Stoll and H. Preuss, *Chem. Phys. Lett.*, 1989, **157**, 200–205.

15 (*a*) R. Ditchfield, W. J. Hehre and J. A. Pople, *J. Chem. Phys.*, 1971, **54**, 724–728; (*b*) W. J. Hehre, R. Ditchfield and J. A. Pople, *J. Chem. Phys.*, 1972, **56**, 2257–2261; (*c*) P. C. Hariharan and J. A. Pople, *Mol. Phys.*, 1974, **27**, 209–214; (*d*) M. S. Gordon, *Chem. Phys. Lett.*, 1980, **76**, 163–168; (*e*) P. C. Hariharan and J. A. Pople, *Theor. Chim. Acta*, 1973, **28**, 213–222; (*f*) M. M. Francl, W. J. Pietro, W. J. Hehre, J. S. Binkley, D. J. DeFrees, J. A. Pople and M. S. Gordon, *J. Chem. Phys.*, 1982, **77**, 3654–3655; (*g*) R. C. Binning Jr. and L. A. Curtiss, *J. Comput. Chem.*, 1990, **11**, 1206–1209; (*h*) V. A. Rassolov, J. A. Pople, M. A. Ratner and T. L. Windus, *J. Chem. Phys.*, 1998, **109**, 1223–1229; (*i*) V. A. Rassolov, M. A. Ratner, J. A. Pople, P. C. Redfern and L. A. Curtiss, *J. Comput. Chem.*, 2001, **22**, 976–984.

16 (*a*) S. Mori and E. Nakamura, *Chem.–Eur. J.*, 1999, **5**, 1534–1543; (*b*) M. Alcamí, A. Luna, O. Mó, M. Yáñez, J. Tortajada and B. Amekraz, *Chem.–Eur. J.*, 2004, **10**, 2927–2934; (*c*) R. Shang, Y. Fu, Y. Wang, Q. Xu, H. Z. Yu and L. Liu, *Angew. Chem., Int. Ed.*, 2009, **48**, 9350–9354; (*d*) M. Yamanaka, A. Inagaki and E. Nakamura, *J. Comput. Chem.*, 2003, **24**, 1401–1409; (*e*) S. Mori, E. Nakamura and K. Morokuma, *J. Am. Chem. Soc.*, 2000, **122**, 7294–7307; (*f*) M. R. A. Blomberg, P. E.M. Siegbahn, G. T. Babcock and M. Wikström, *J. Am. Chem. Soc.*, 2000, **122**, 12848–12858; (*g*) H. Zhao, L. Dang, T. B. Marder and Z. Y. Lin, *J. Am. Chem. Soc.*, 2008, **130**, 5586–5594; (*h*) A. Poater, X. Ribas, A. Llobet, L. Cavallo and M. Solà, *J. Am. Chem. Soc.*, 2008, **130**, 17710–17717; (*i*) N. Yoshikai, S. L. Zhang and E. Nakamura, *J. Am. Chem. Soc.*, 2008, **130**, 12862–12863; (*j*) E. Nakamura, S. Mori and K. Morokuma,, *J. Am. Chem. Soc.*, 1997, **119**, 4900–4910; (*k*) P. Brandt, M. J. Södergren, P. G. Andersson and P. O. Norrby, *J. Am. Chem. Soc.*, 2000, **122**, 8013–8020; (*l*) J. I. García, G. Jiménez-Osés, V. Martínez-Merino, J. A. Mayoral, E. Pires and I. Villalba, *Chem.–Eur. J.*, 2007, **13**, 4064–4073; (*m*) H. Z. Yu, Y. Y. Jiang, Y. Fu and L. Liu, *J. Am. Chem. Soc.*, 2010, **132**, 18078–18091.

17 M. Cossi, G. Scalmani, N. Rega and V. Barone, *J. Chem. Phys.*, 2002, **117**, 43–54.

18 M. J. Frisch, G. W. Trucks *et al.*, *Gaussian 03*, Revision B.05; Gaussian, Inc., Pittsburgh, PA, 2003 (full citation of Gaussian 03 is available in the ESI†).

19 (*a*) J. P. Blaudeau, M. P. McGrath, L. A. Curtiss and L. Radom, *J. Chem. Phys.*, 1997, **107**, 5016–5021; (*b*) M. M. Francl, W. J. Pietro, J. S. Hehre, W. J. Binkley, D. J. DeFrees, J. A. Pople and M. S. Gordon, *J. Chem. Phys.*, 1982, **77**, 3654–3665.

20 (*a*) J. I. Seeman, *J. Chem. Educ.*, 1986, **63**, 42–48; (*b*) J. I. Seeman, *Chem. Rev.*, 1983, **83**, 84–134.

21 H. Shimizu, D. Igarashi, W. Kuriyama, Y. Yusa, N. Sayo and T. Saito, *Org. Lett.*, 2007, **9**, 1655–1657.

22 (*a*) P. W. N. M. V. Leeuwen, P. C. J. Kamer, J. N. H. Reek and P. Dierkes, *Chem. Rev.*, 2000, **100**, 2741–2769; (*b*) C. P. Casey, G. T. Whiteker, M. G. Melville, L. M. Petrovich, J. A. Gavney Jr. and D. R. Powell, *J. Am. Chem. Soc.*, 1992, **114**, 5535–5543; (*c*) C. J. Cobley, R. D. J. Froese, J. Klosin, C. Qin and G. T. Whiteker, *Organometallics*, 2007, **26**, 2986–2999.

23 Pd: (*a*) K. Selvakunar, M. Valentini and P. S. Pregosin, *Organometallics*, 2000, **19**, 1299–1307; (*b*) P. Dotta, P. G. A. Kumar and P. S. Pregosin, *Organometallics*, 2004, **23**, 2295–2304; (*c*) G. Trabesinger, A. Albinati, N. Feiken, R. W. Kunz, P. S. Pregosin and M. Tschoerner, *J. Am. Chem. Soc.*, 1997, **119**, 6315–6323. Rh: (*d*) D. S. Clyne, Y. C. Mermet-Bouvier, N. Nomura and T. V. Rajanbabu, *J. Org. Chem.*, 1999, **64**, 7601–7611; (*e*) T. V. Rajanbabu, T. A. Ayers and A. L. Casalnuovo, *J. Am. Chem. Soc.*, 1994, **116**, 4101–4102. Ru: (*f*) K. Mikami, T. Korenaga, M. Terada, T. Ohkuma, T. Pham and R. Noyori, *Angew. Chem.*, 1999, **111**, 517–519. Ir: (*g*) H. U. Blaser, H. P. Buser, H. P. Jalet, B. Pugin and F. Spindler, *Synlett*, 1999, **4**, 867–868.

